IOP Conf. Series: Materials Science and Engineering **278** (2017) 012053 doi:10.1088/1757-899X/278/1/012053

Parametric study on the thermal performance of beam screen samples of the High-Luminosity LHC upgrade

P Borges de Sousa, M Morrone, N Hovenga, C Garion, R van Weelderen, T Koettig and J Bremer

CERN, CH-1211 Geneva 23, Switzerland

E-mail: pat.borges.sousa@cern.ch

Abstract. The High-Luminosity upgrade of the Large Hadron Collider (HL-LHC) will increase the accelerator's luminosity by a factor 10 beyond its original design value, giving rise to more collisions and generating an intense flow of debris. A new beam screen has been designed for the inner triplets that incorporates tungsten alloy blocks to shield the superconducting magnets and the 1.9 K superfluid helium bath from incoming radiation. These screens will operate between 60 K and 80 K and are designed to sustain a nominal head load of 15 W m^{-1}, over 10 times the nominal heat load for the original LHC design. Their overall new and more complex design requires them and their constituent parts to be characterised from a thermal performance standpoint. In this paper we describe the experimental parametric study carried out on two principal thermal components: a representative sample of the beam screen with a tungsten-based alloy block and thermal link and the supporting structure composed of an assembly of ceramic spheres and titanium springs. Results from both studies are shown and discussed regarding their impact on the baseline considerations for the thermal design of the beam screens.

1. Introduction

In the framework of the High-Luminosity upgrade of the LHC, new screens have been designed for the inner triplets Qx and for D1 (quadrupoles and dipole in the insertion regions) [1]. Among other functions, the beam screen is needed to shield the superconducting magnets and the 1.9 K superfluid helium bath from the incoming radiation caused by the collisions. The new design for the beam screen sees a substantial increase in complexity from its LHC counterpart as well as a different operating temperature range; a comparison of both beam screen parameters is given in table 1. The need for shielding material and the higher heat loads lead to the design shown in figure 1.

The beam screens are inserted in the cold bore of the superconducting magnets. They are mainly composed of an octagonal inner beam screen, tungsten alloy absorbers, cooling tubes, a series of thermal links and a supporting structure, which mechanically holds the assembly while minimising thermal contact to the cold bore and ensuring proper alignment.

The screen is made out of 1 mm-thick stainless steel with its inner surface coated with an 80 µm copper layer. This highly conductive layer minimises the power dissipated by the beam image currents and the impedance seen by the beam. The screen features pumping slots to allow

Table 1. Cooling scheme characteristics of the LHC and HL-LHC beam screens [2, 3].

	LHC beam screen	HL-LHC beam screen
Operating temperature	4.6 K to 20 K	60 K to 80 K
Nominal heat load	$\approx 1\,\mathrm{W\,m^{-1}}$	$15\,\mathrm{W\,m^{-1}}$ (D1, Q2, Q3), $25\,\mathrm{W\,m^{-1}}$ (Q1)
Cooling fluid	supercritical He	supercritical He
Operating pressure	3 bar	20 bar
Mass flow rate	$1\,\mathrm{g\,s^{-1}}$	$10\,\mathrm{g\,s^{-1}}$ to $20\,\mathrm{g\,s^{-1}}$
Absorber material	none	tungsten alloy

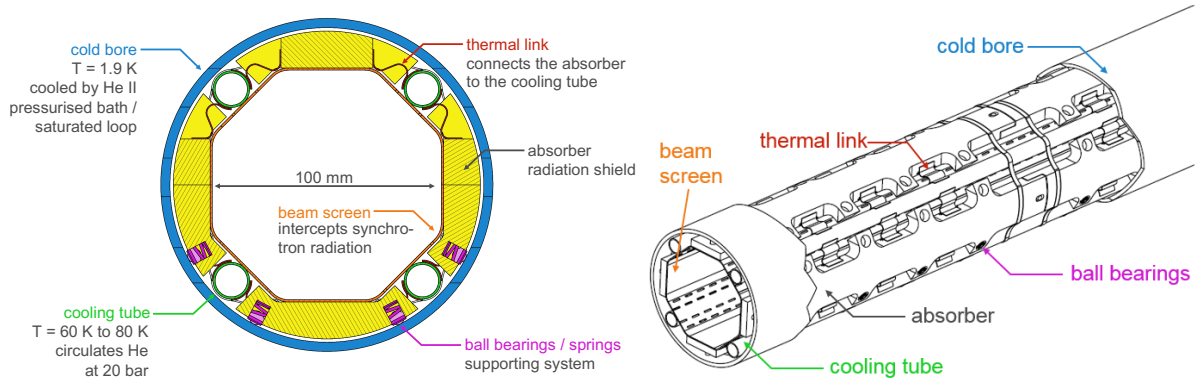

Figure 1. Cross-section and isometric views of the inner triplets beam screen inserted into the cold bore, depicting the various components; adapted from [4].

for cryopumping of gas molecules remaining in the beam tube by the cold bore at 1.9 K. Each section of the beam screen is 0.4 m long (*i.e.* a full absorber block length).

The absorbers are blocks made out of a heavy tungsten-based alloy (95% W, 3.5% Ni, 1.5% Cu; thickness 16 mm for Q1 and 6 mm for the other triplets and D1 [4], referred to as "tungsten" throughout this paper), which combines the radiation shielding properties of tungsten with a high thermal conductivity, in addition to being non-magnetic [4]. These shielding blocks are responsible for absorbing most of the incoming debris caused by beam-beam collisions and rest on the beam screen outer surface.

There are four cooling tubes along the beam screen, made out of 1 mm-thick stainless steel ($\varnothing_o = 16$ mm for Q1 and $\varnothing_o = 10$ mm for D1, Q2 and Q3). These tubes are spot-welded to the beam screen, providing cooling to both the screen (directly) and the tungsten block (via the thermal links). A supercritical helium flow at 20 bar will circulate inside the cooling tubes at a mass flow rate of around $11\,\mathrm{g\,s^{-1}}$; the temperature can vary from 60 K up to 75 K along the total length of the beam screen.

The thermal links connect the tungsten blocks to the cooling tube. They are made out of ten 100 µm sheets of Cu RRR 100 with a total cross-section of $3\,\mathrm{mm^2}$. They are directly brazed to the tungsten block on one side and to a pad on the other, which in turn is welded to the cooling tube. This pad is made out of stainless steel with an 80 µm copper layer, and its purpose is to ensure a weldable surface to the cooling tube while providing a better distribution of the incoming heat load onto its surface.

The supporting structure consists of a series of zirconium oxide (ZrO_2) spheres resting on 3D-printed titanium springs. ZrO_2 combines excellent mechanical properties with a low thermal conductivity [5]. These spheres are the only point of contact between the beam screen and the cold bore (32 per section, $\varnothing 6$ mm for Q1 and $\varnothing 4$ mm for D1 and the other triplets).

The main requirement for the beam screens is that for the nominal heat load ($25\,\mathrm{W\,m^{-1}}$

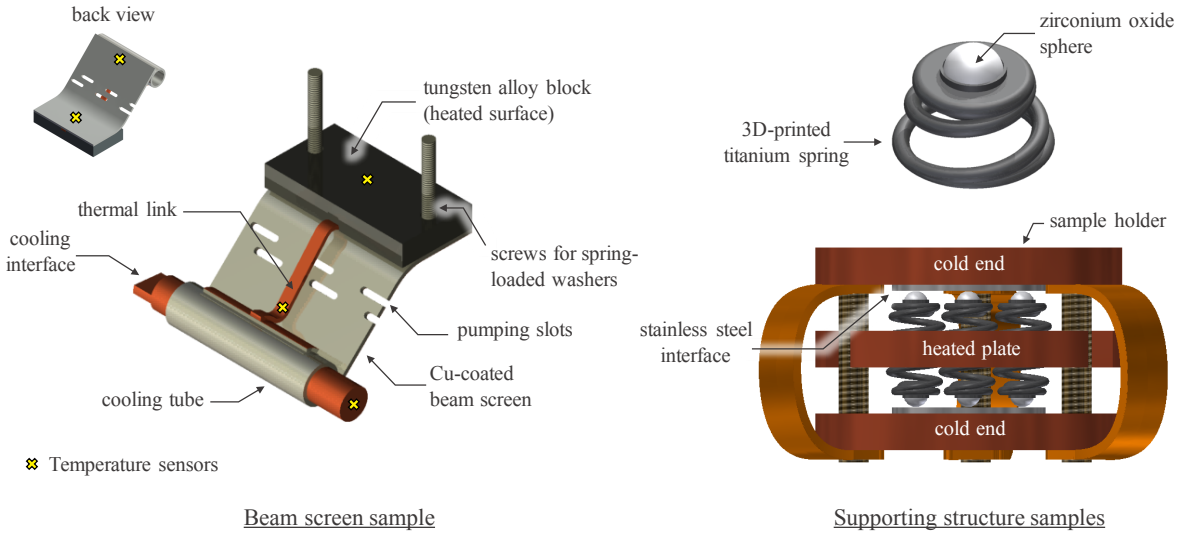

Figure 2. Drawing of portions of the beam screen selected as representative of the assembly for the thermal performance studies, with the corresponding identification of the individual components.

for Q1 and 15 W m^{-1} for Q2, Q3 and D1) the temperature of the internal copper layer of the screen should not increase by more than the requested 5 K with respect to the temperature of the supercritical helium circulating in that section of the screen, following [3]. Although there is no specific limit imposed on the tungsten block temperature, it should be evaluated and kept below reasonable values so that the heat transferred to the 1.9 K cold bore either by radiation or by conduction through the supporting structure is minimised and particle desorption is kept to a minimum.

The parametric study reported here consisted of two parts: the first part aimed to characterise the beam screen itself and evaluate the influence of different parameters such as compression force between the tungsten block and the screen, the heat load and the base temperature on the inner screen temperature. The second part focused on assessing the thermal conductance of the supporting spring components in order to estimate the heat load reaching the 1.9 K cold bore.

2. Sample geometries and test set-up

A representation of both samples is shown in figure 2; for its relative location to the cold bore and screen refer to figure 1. The sample has been manufactured specifically for this study and consists of a 40 mm-long portion of the beam screen (representative of the design for Q2) with a 40 mm × 20 mm × 6 mm slab of tungsten resting on the screen, aligned by two threaded rods.

Each sample was instrumented with six temperature probes, placed on the tungsten block, on two points on the beam screen, on the thermal link, on the cooling tube and on the heat sink. To apply a compression force on the tungsten block, two spring-loaded washers were mounted on a set of screws attached to the beam screen itself. The springs press the tungsten block against the beam screen with a nominal compression calculated to be 1.82 N.

The heat load applied on the block's surface ranged from 0 mW to 400 mW, representing 0 W m^{-1} to 25 W m^{-1} on the beam screen; this was calculated by considering that each 0.4 m section of beam screen assembly contains four tungsten blocks each with six thermal links; for a 25 W m^{-1} heat load each thermal link needs to transfer $\dot{Q} = 25 \times \frac{0.4}{6\times4} = 417$ mW from the tungsten block to the cooling tube.

Measurements of the supporting springs were carried out for a sample representative of Q2 magnets (ZrO_2 spheres of 4 mm diameter). A set of six springs was assembled onto a sample

Table 2. Measured maximum temperature increase of relevant beam screen components for a Q2-type magnet, for a nominal heat load of $15\,\mathrm{W\,m^{-1}}$.

	Nominal compression		No compression	
Base T	W block ΔT	Beam screen ΔT	W block ΔT	Beam screen ΔT
(60.00 ± 0.16) K	(14.00 ± 0.06) K	(3.20 ± 0.04) K	(13.50 ± 0.06) K	(2.20 ± 0.04) K
(75.00 ± 0.23) K	(14.00 ± 0.09) K	(3.40 ± 0.03) K	(13.50 ± 0.09) K	(2.30 ± 0.03) K

holder (as shown in figure 2) in a symmetrical configuration so that the heated side of the springs is thermally decoupled from the rest of the set-up, heat transfer occurs only through the springs+sphere set. The ZrO_2 spheres are in contact with a stainless steel plate that simulates the cold bore. Heat losses through the cabling wires for the electric heater and temperature sensor were taken into account and compensated for.

Measurements were carried out using a Sumitomo Heavy Industries two-stage pulse tube refrigerator (PTR) that can provide up to 1 W of cooling power at 4.2 K on the second stage and a no-load temperature of 2.6 K. A detailed description of the measurement set-up can be found in [6].

3. Results and discussion

Results are divided into the evaluation of the beam screen thermal pathways and into the thermal conductance measurements of the supporting structure in contact with the cold bore.

3.1. Beam screen thermal pathways

Temperatures were measured on the beam screen sample while varying the following parameters:

- Base temperature (*i.e.* helium gas circulating in the cooling tube) from 50 K to 80 K;
- Heat load on tungsten block from 0 mW to 400 mW ($\approx 0\,\mathrm{W\,m^{-1}}$ to $25\,\mathrm{W\,m^{-1}}$);
- Compression force, measured without compression and 1.82 N nominal compression.

From these measurements, the most relevant results are the ones obtained for the nominal heat load of $15\,\mathrm{W\,m^{-1}}$ on the beam screen inner surface and on the tungsten block. Table 2 shows the maximum temperatures observed for the referred components for both nominal and no compression, for the base cooling temperature at the start of the inner triplets at 60 K and and its end at 75 K, originated from the maximum temperature margin (80 K − 5 K) for the beam screen.

Results show a maximum tungsten block temperature increase of 14 K for the nominal heat load that does not change significantly with either the base temperature or compression. Regarding the beam screen, temperatures were measured at two points on its inner surface: one directly below the tungsten block and another close to where the cooling tube is welded; the first case represents the highest temperature increase (see figure 2, beam screen sample back view). We recorded a maximum temperature increase of 3.4 K on the beam screen for nominal compression and at the highest base temperature (*i.e.* towards the end of the inner triplet section); this difference decreases to 2.3 K if no compression force is present. In any case, these values are well below the required 5 K maximum ΔT between the cooling fluid circulating in the tubes (base temperature) and the inner surface of the beam screen, meaning that this design satisfies the temperature requirements.

Beyond the temperature increase of the beam screen components depending on base temperature, heat load and compression force, it is interesting to analyse the existing

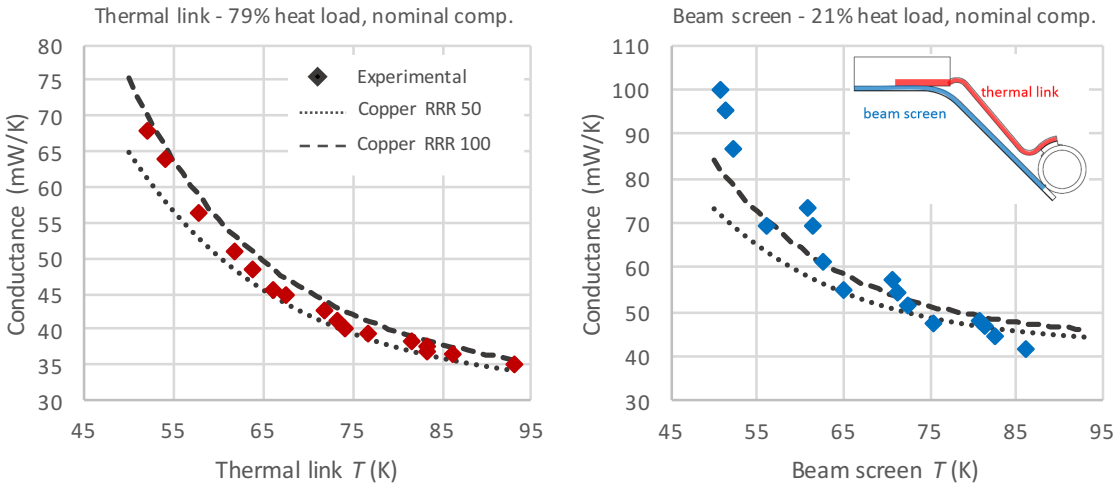

Figure 3. Thermal conductance of the thermal link and the beam screen (no interfaces) as a function of temperature. Lines represent calculated values for conductance and points are experimental data considering a fraction $x = 79\%$ of the heat load through the link and $(1 - x) = 21\%$ through the beam screen. Legend applies for both plots.

thermal pathways and assess the different contributions to heat transfer, and identify possible bottlenecks. Two paths for heat transfer from the tungsten block to the cooling tube are identified:

- Thermal link pathway: includes the tungsten block-Cu link brazed joint, thermal link itself, Cu-covered stainless steel pad and weld to the cooling tube, see figure 2;
- Beam screen pathway: includes the tungsten block-beam screen contact interface, the Cu-covered stainless steel beam screen, and the welded joint of the beam screen to the cooling tube.

Since the objective is that the majority of the heat flows through the thermal link, identifying a bottleneck on this pathway can lead to improvements that further increase its conductance. Inversely, the heat transfer from the tungsten block to the beam screen should be minimised, but any heat that does arrive at the screen should be efficiently evacuated to the heat sink.

First it was necessary to determine what percentage of the total applied heating power is effectively transferred through each pathway. For this reason, the beam screen and thermal link conductances are calculated analytically and the experimental ratio of the thermal pathways results is adjusted regarding the distribution of heat load. The results from this exercise are shown in figure 3. The conductance of the thermal link was calculated with a 1D model taking into account its geometry ($L = 40\,\text{mm}$ and $A = 3\,\text{mm}^2$) for Cu RRR 50 and 100, while the beam screen conductance considered both Cu and stainless steel layers and a more complex geometry that accounts for an average cross section due to the pumping slots cut-outs.

Calculated and experimental values agree if we consider that 21% of the total heat load flows through the beam screen (*i.e.* 79% of heating power transferred through the thermal link); this ratio shifts to 89%-11% for no compression. Results show a decreasing conductance with increasing temperature of the thermal link between 50 K and 90 K, which is expected for a link made out of copper, but this behaviour is also evident for the beam screen, indicating that the thin copper layer is also dominating the heat transfer on the screen. Conductance values for both components are similar since only the solid part is considered and not the thermal pathway complete with interfaces; in fact, the cross-section of the copper layer on the screen is marginally

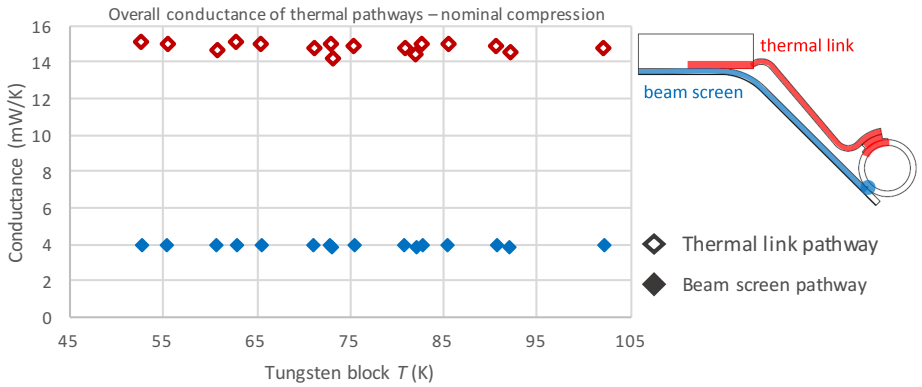

Figure 4. Overall thermal conductance of the two major thermal pathways for nominal compression, considering that 21% of the heat load is transferred through the beam screen.

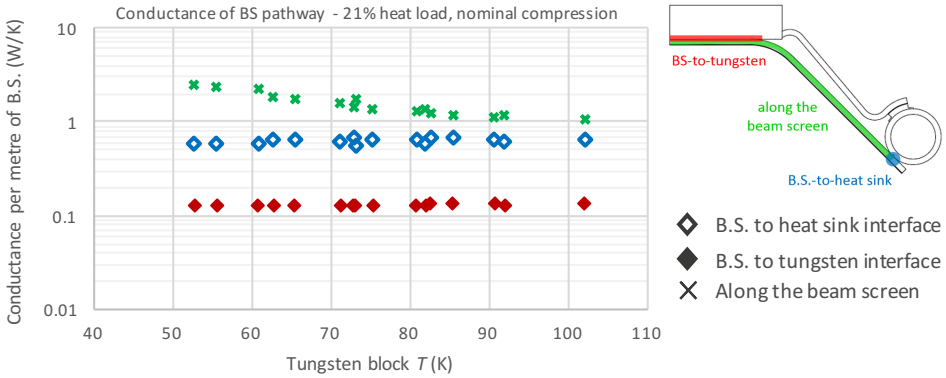

Figure 5. Thermal conductance along the beam screen pathway as a function of the tungsten block temperature, nominal compression applied (values shown in $\mathrm{W\,K^{-1}}$ per meter of screen).

larger than the cross-section of the thermal link. Figure 4 shows the overall conductance for both pathways, now including the interfaces.

The overall conductance of the two thermal pathways evidences the differences in heat transfer: the conductance of the thermal link and beam screen pathways (*i.e.* taking into account the contact resistance and welded joints between the different components) differs of almost a factor 4. The fact that the results are constant with temperature, unlike the conductance of the individual components as shown in figure 3, shows that the material and contact thermal conductances are of the same magnitude over the measured temperature range on either thermal pathway. This is expected as a design feature, since the individual components themselves should not be the limiting factor for heat transfer. The beam screen pathway has an overall thermal conductance of around $4\,\mathrm{mW\,K^{-1}}$ while the thermal link is between $14\,\mathrm{mW\,K^{-1}}$ and $16\,\mathrm{mW\,K^{-1}}$. To understand where this difference in effective conductance comes from we must look at the individual conductance values for the components of each pathway. Figure 5 and figure 6 show the breakdown of the conductance values for each part of the beam screen and thermal link pathways, respectively.

The results for the beam screen demonstrate that the interfaces to other components are responsible for the low thermal conductance: the spot-welded joint of the beam screen to the cooling tube presents a thermal conductance twice as low as the beam screen itself, and the compressed contact between the screen and the tungsten block surface are over an order of magnitude lower at around $0.1\,\mathrm{W\,K^{-1}}$ (see figure 6). As expected, the restriction on the beam

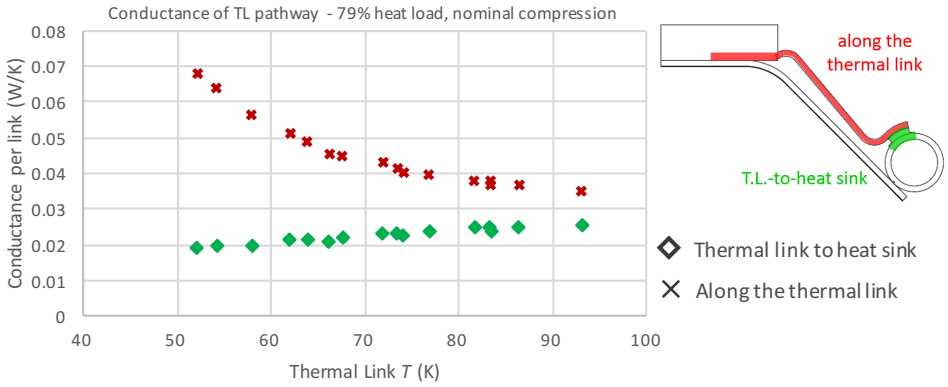

Figure 6. Conductance along the thermal link pathway as a function of the link temperature, nominal compression applied (values shown in $\mathrm{W\,K^{-1}}$ per link).

screen is the contact resistance between the tungsten block and the stainless steel surface of the screen. This interface is intended to have a low conductance and the measured values are low enough that no effort was made in lowering it further. Measurements with no compression force show overall little change in this interface behaviour (from $0.1\,\mathrm{W\,K^{-1}}$ with nominal compression to $0.06\,\mathrm{W\,K^{-1}}$ with no compression).

Regarding the thermal link pathway, the conductance of the link itself and the brazed points to the pad and cooling tube have comparable high values, meaning that this interface does not constitute a significant bottleneck for heat transfer. The thermal link has a higher conductivity at lower temperatures in the studied range, but at temperatures higher than 80 K conductance values converge. The interface resistance between the tungsten block and the thermal link was considered negligible due to the conductivity of the tungsten alloy being relatively high [4] and due to the quality of the brazed contact.

3.2. Supporting structure conductance

The supporting structure made up of zirconium oxide spheres and titanium springs was characterised for both the nominal compression (7.5 N) and twice this value (15 N). Figure 7 shows the results, both in terms of conductance and heat load transferred to the cold bore per spring assembly, as a function of the hot side (*i.e.* tungsten block) temperature. For every measurement, the cold end temperature was maintained between 2.7 K and 3 K, value limited by cryocooler performance.

The overall conductance increases with increasing temperature, although with a reduced slope for temperatures higher than 80 K where it reaches values in the range of $0.08\,\mathrm{mW\,K^{-1}}$. Although there is an increase in thermal conductance as the compression force is increased as expected for a sample with multiple interfaces [7], it can be considered negligible since an increase in force by a factor 2 results in little more than a 10% increase in conductance up to the 80 K temperature range. The heat load transferred from the tungsten block to the cold bore surface through the springs varies between 5 mW and 7 mW per spring for the operating temperature range of the tungsten block ($\approx$ 75 K to 95 K). This means that a complete 0.4 m section of the beam screen can transfer up to $7 \times 32 = 224$ mW to the cold bore, resulting in a maximum of 560 mW per meter of beam screen if all the available spring assemblies are taken into account. However, the current baseline configuration considers using the supporting structures only on the bottom half of the beam screen, resulting in a heat load of 280 mW per meter of beam screen. This heat load is only the one conducted from the beam screen to the cold bore through the springs, and excludes the additional load radiated by the blocks.

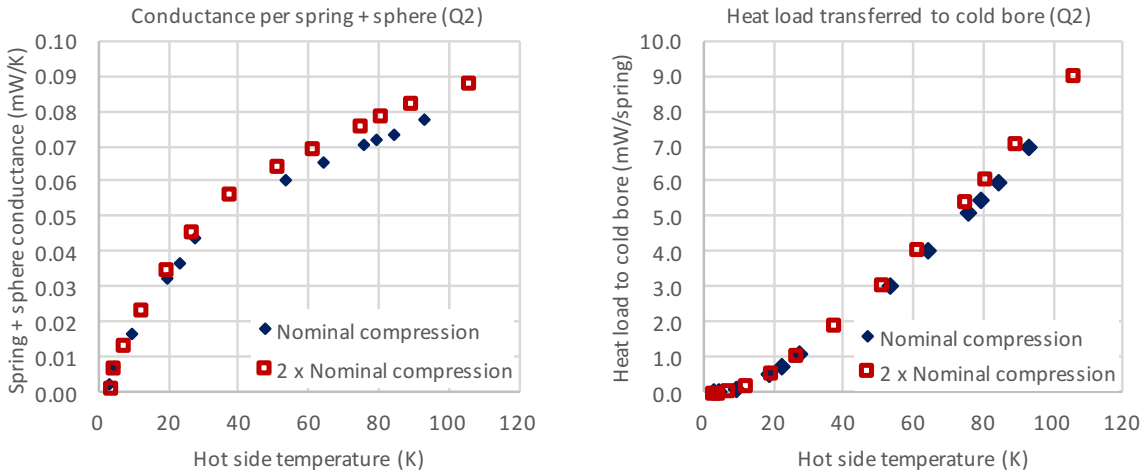

Figure 7. Conductance per spring (Q2) as a function of the tungsten block temperature (left) and respective heat load transferred to the cold bore (right).

4. Conclusion

Results for the beam screen sample show that for the nominal heat load of 15 W m^{-1} the 5 K temperature difference between the inner surface of the beam screen and the cooling source is never exceeded – the highest temperature difference measured on the beam screen was 3.4 K at the nominal load and compression. The two major thermal pathways, the beam screen and the thermal link, were characterised regarding their overall conductance. It was shown that, even with no compression, there is still ≈10% of the total heat load being transferred through the beam screen, rising to ≈20% when the nominal compression force is applied. On the thermal link side, the effective conductance of the thermal pathway is limited by the interface resistance between the pad and the welding to the cooling tube. The connection between the copper link and the tungsten block shows virtually no resistance and can be neglected. On the beam screen side, the restriction to heat transfer is clearly the contact resistance between the tungsten block and the beam screen surface, either under no or nominal compression, which is desired since it thermally decouples the inner surface of the screen from the absorbers.

The supporting system for the beam screens was characterised regarding its thermal conductance. Compression force was found to have little influence (less than 10%) in the overall conductance, which is around 0.08 mW K^{-1} for the 75 K to 95 K range. This means a maximum heat load transferred to the 1.9 K cold bore of 560 mW per meter of beam screen needs to be considered, whereas the current baseline configuration brings this value down to 280 mW per meter of beam screen since only the bottom half of the screen is fitted with the supports.

References

[1] Garion C, Baglin V and Kersevan R 2015 *Proc. 6th International Particle Accelerator Conference* 60–63
[2] Hatchadourian E, Lebrun P and Tavian L 1998 Supercritical Helium Cooling of the LHC Beam Screens Tech. Rep. LHC Project Report 212
[3] Kersevan R, Garion C and Kos N 2014 Preliminary Design of the HiLumi-LHC Triplet Area Beam Screen Tech. Rep. CERN-ACC-2014-0268
[4] Garion C, Dufay-Chanat L, Koettig T, Machiocha W and Morrone M 2015 *IOP Conference Series: Materials Science and Engineering* **102** 012013
[5] Maciocha W and Koettig T 2014 Thermal conductivity measurement report: Zirconium oxide Tech. Rep. CERN EDMS document 1845273 URL `https://edms.cern.ch/document/1845273/1`
[6] Koettig T, Maciocha W, Bermudez S, Rysti J, Tavares S, Cacherat F and Bremer J 2017 *IOP Conference Series: Materials Science and Engineering* **171** 012103
[7] Gmelin E, Asen-Palmer M, Reuther M and Villar R 1999 *Journal of Physics D Applied Physics* **32** R19–R43